

07,04

On the issue of deformation and destruction of porous ceramics based on diatomite

© A.A. Skvortsov, V.K. Nikolaev, M.N. Luk'yanov, I.E. Chebeneva

Moscow Polytechnic University,
Moscow, Russia

E-mail: skvortsovaa2009@yandex.ru

Received September 27, 2022

Revised October 11, 2022

Accepted October 14, 2022

The presented work is devoted to the study of deformation and destruction of porous ceramics based on diatomite. The dependences of the elastic modulus of the material on porosity were obtained by scanning electron microscopy, mechanical compression tests of samples and acoustic emission method: with a change in the porosity of the medium in the range of 20–60%, the value of the elastic modulus varied in the range from 240 to 50 MPa. It was also found that the tensile strength of the material's changes by ~ 10 MPa with a change in porosity.

Keywords: porous ceramics, diatomite, modulus of elasticity, tensile strength, porosity, fracture mechanics.

DOI: 10.21883/PSS.2023.01.54985.485

1. Introduction

Porous ceramics today are among the most promising objects from the point of view of engineering new materials [1]. When designing materials, firstly, the characteristics of the porous structure itself are taken into account, and secondly, that the formed pores should ensure the achievement of the specified physical and mechanical characteristics of the medium. Thus, the pores in the material should be considered as a functional phase of [1,2].

When loaded, the pore system undergoes significant changes, thereby affecting the strength and plasticity of the entire material [2]. In this case, the pores are discontinuities that reduce the strength properties of the material and are an effective stress relaxation site.

The deformation behavior of ceramic materials under the action of an external load can be characterized as linear elastic [3]. The presence of a porous structure in ceramics leads, as a rule, to a change in the nature of deformation. For such materials, nonlinear laws of the relationship between stress and deformation are characteristic [4], i.e., in addition to elastic deformation, micro-damage accumulates in the form of local destruction of the ceramic frame. At the same time, after removing external loads, the development of cracks stops.

Due to the developed porous structure, ceramics are used in areas related to thermal insulation (as a rule, such media have low values of the thermal conductivity coefficient $\lambda < 0.2$ W/(m · K)). Materials with low thermal conductivity due to high porosity ($P = 10\text{--}90\%$), it is used for thermal insulation of building structures and industrial equipment. Products with a density of $\rho > 400$ kg/m³ are used as structural and thermal insulation materials.

In a wide range of thermal insulation materials, ceramic materials occupy a significant place with the possibil-

ity of using them at temperatures of insulated surfaces over 1000°C [1]. One of such materials is foam-diatomite ceramics. The basis of this material is diatomite, which is a sedimentary rock consisting mainly of shells of diatoms. Individual diatom flaps (up to 0.2 mm in diameter) with micro- and nanopores form the structure of the material. Chemically, diatomite consists of 96% aqueous silica and has high porosity, low thermal and sound conductivity, refractory and acid resistance.

Lately, along with the traditional use of diatomite ceramics (filtration and thermal protection), there has been information about new, rather unexpected applications of it. For example, in [5], the possibility of developing effective materials based on diatomite ceramics that protect against electromagnetic interference is shown. The authors used artificially grown skeletons of diatoms obtained from porous silica, which were immersed in solutions of $\text{Ti}_3\text{C}_2\text{T}_x$ with subsequent annealing in argon medium. The electromagnetic interference coefficient of the obtained composites reached a maximum electromagnetic interference coefficient of 43.2 dB in the X-range and compressive strength of 67.5 MPa, establishing a unique balance of mechanical characteristics and shielding characteristics. In [6], sintered nanoporous diatomite ceramics were used as a new biomaterial with a significant ability to cell growth and bone mineralization. The biomaterial was made by sintering diatoms at various pressures and temperatures (up to 1100°C). The biocompatibility of the biomaterial with *in vitro* cells was initially evaluated using human cells. These cells were attached to the biomaterial, and in fact it was observed that they mainly grew on diatom biomaterial in a higher density than on commercial cell culture plates [6]. The fact that diatom shells are promising for bone tissue engineering, since silicon enhances bone regeneration, was reported earlier [7]. The study of a new protective coating

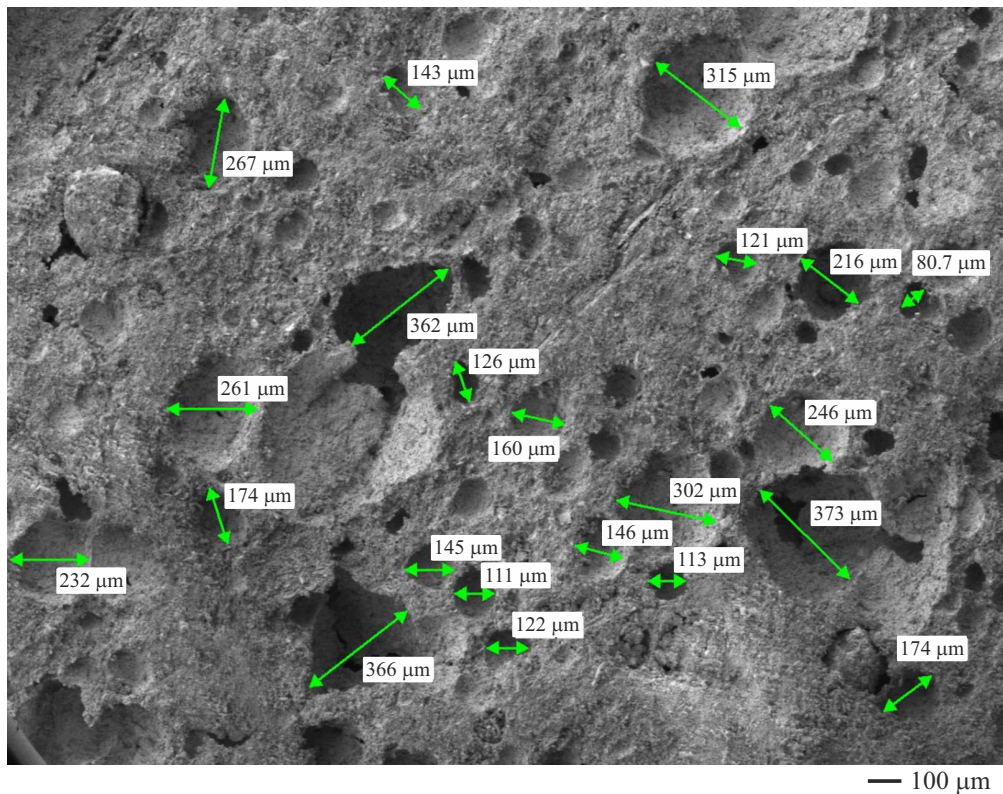


Figure 1. SEM-photo of the sample surface with pore sizes.

(and its various physicochemical properties) for orthopedic magnesium implants was carried out in work [8]. The coating was synthesized by microarc oxidation, and the electrolyte solution was doped with diatomite particles. The results of the studies showed that the corrosion resistance of the coated samples was about three orders of magnitude higher than that of the original Mg alloy sample. In addition, such a coating significantly reduced the cytotoxic effect of *in vitro* on cells, which makes it a promising biogenic tool for increasing the biocompatibility of implants based on Mg [8].

Thus, the range of applications of diatomite-based materials has significantly expanded in recent years: from biotechnology, to the mechanics of materials, including micro-sensory technology associated with the creation of micro-devices with specific characteristics [9,10]. That is why the study of the mechanical properties of diatomite ceramics from porosity, including the features of its destruction, seems to be an urgent task.

2. Materials and research techniques

Molded samples of diatomite ceramics in the form of parallelepipeds with a size of $15 \times 15 \times 100$ mm with a porosity of 20–60% and a range of operating temperatures of up to 900°C were used as a material for research. Its production was carried out according to standard technology, including drying of the rock, crushing, formation of the flask with the addition of a foamer and roasting [1,11].

The composition of the samples was analyzed using a high-resolution auto-emission scanning electron microscope JSM 7500F (JEOL, Japan) equipped with an OxfordX-Max80 EMF detector with a SATW window (at accelerating voltage 1 and 20 kV and beam current 1 nA). The sensitivity of the device was 0.2–1 at.% depending on the element. The spatial resolution was not less than 1 nm, the pressure in the sample chamber during the survey — not higher than $9.6 \cdot 10^{-5}$ Pa. The pore size in ceramics and the distance between before and after compression tests were measured on the sample section using a scanning electron microscope. Up to 5 microphotographs and at least 200 pores were analyzed for each sample (Fig. 1).

Mechanical tests of compression samples were carried out on a testing machine at a speed of 1 mm/min with a record of loading curves, which determined the tensile strength and relative deformation of the material [11]. It is known that the value of the static modulus of elasticity E_s of quartz ceramic samples (as well as other types of ceramics) depends on the geometry and porosity P of the samples under study [12]. Therefore, during the experiments, the sizes of our samples and porosity were strictly controlled ($E_{s,0}$ — elastic modulus at zero porosity).

For diatomite, all samples remained in the form of parallelepipeds throughout the test. The destruction occurred suddenly when the maximum load σ_{\max} was reached with the appearance of a number of inclined cracks located approximately at an angle 45° to the forming lateral surfaces

of the sample, i.e. along the lines of action of maximum tangential stresses. The compressive strength was also determined by compression diagrams (Fig. 2).

To further study the dynamics of material deformation, the acoustic emission (AE) method was used, which is actively used to monitor the destruction of various materials (in t.h. and rocks) in real time, including the prediction of dangerous dynamic phenomena in coal mines [13]. Today, in combination with modern methods of digital signal processing, AE is an important tool in the study of diagnostics of porous materials, including nonlinear deformations, changes in the propagation velocities of elastic waves and their attenuation [14].

AE signals were recorded by a piezoelectric sensor mounted on the surface of the plate under study. A piezoceramic plate of lead zirconate-titanate (PZT) with a thickness of 0.3 mm and a diameter of 10 mm, whose natural frequencies ($f_i \geq 4$ MHz) were significantly higher than the spectral composition of the response signal, acted as a sensor. The electrical response from the $U(t)$ sensor was fed to a digital oscilloscope with the ability to record information. Spectral composition of the signal-response $U(\omega)$ was obtained using the standard fast Fourier transform

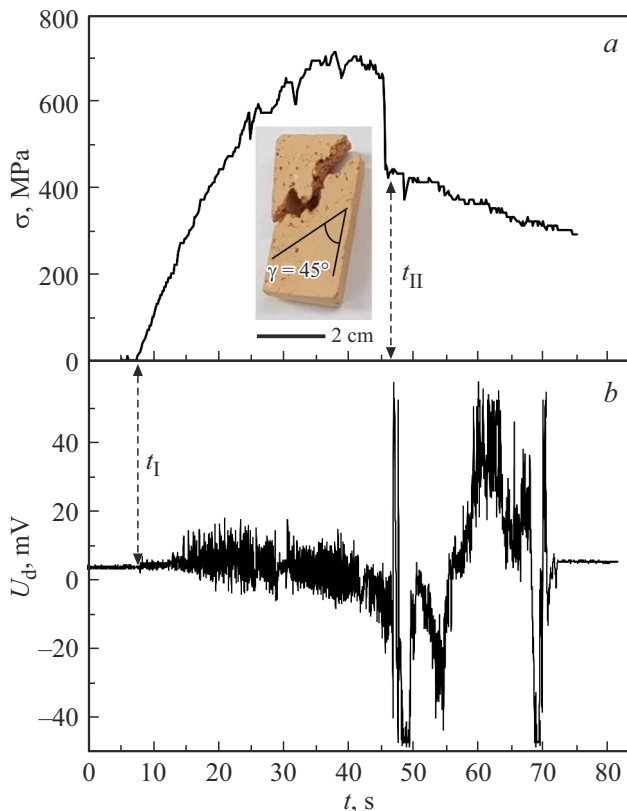


Figure 2. *a* — compression diagram of a sample of foam-diatomite ceramics with a porosity of 40% at a rate of 1 mm/min and *b* — signal of acoustic emission during sample compression recorded by a piezoelectric sensor mounted directly on the deformable sample. On the insert: a photo of the sample after compression deformation.

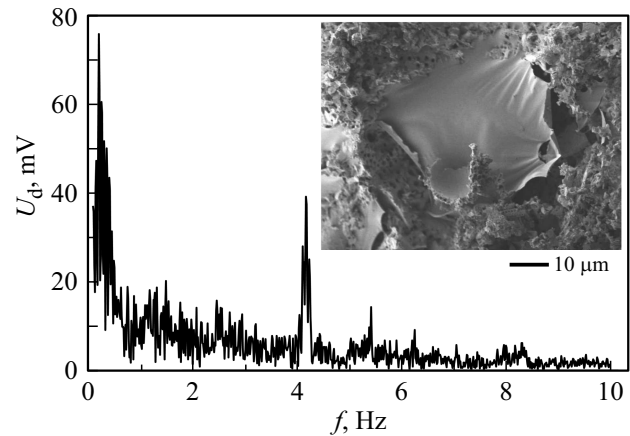


Figure 3. Fourier spectrum of the acoustic emission signal of the sample during compression deformation. On the insert: The SEM photo of a sample with fragments of a zone of intense plastic deformation of a sample of porous diatomite ceramics with a porosity of $P = 40\%$ after its destruction.

algorithm (Fig. 3). The energy of AE signals $W \sim \sum_n U_n^2$ was estimated from the obtained spectra, where U_n — the amplitudes of the harmonics of the experimental spectrum.

3. Analysis of the results obtained

The results of the study of quartz ceramics are known from the literature [12]. Quartz ceramics, like most of its types, is a brittle material at room temperature, for which Hooke's law is fully valid (the material we study is no exception). This dependence was determined by compression diagrams recorded for samples with different porosity (Fig. 4).

It is not difficult to see that the studied samples clearly show a tendency to decrease the modulus E_s with an increase in porosity P . In literature, various dependences of elastic modulus of porous materials E_s on porosity P [1,2,15–18] are given. Examples of one-parameter dependencies with one phenomenological constant are given in the following table.

It can be seen from the table that these dependencies only approximate the change in Young's modulus from porosity, which is reflected in the spread of the correlation coefficient ($r^2 = 0.790–0.876$). It is obvious that there is no single model and, accordingly, a single theoretical dependence that reliably describes the elastic properties of porous materials. For our experimental data, the best agreement was obtained for the exponential dependence (formula 2 in the table), which is shown in Fig. 5. It should also be noted that in our experiments higher values of E_s were obtained in comparison with the data of the works [2,5] (including for materials with high porosity $P \sim 50–60\%$). The observed differences in the values of E_s are associated with the presence of strengthening additives Al_2O_3 and CaO .

Calculated dependences of elastic modulus on porosity

№	Calculated dependencies $E_s(P)$	Literature	b	E_{s0} , MPa	r^2
1	$E_s(P) = E_{s0}(1-P)^b$	[1,2]	3.9	489	0.839
2	$E_s(P) = E_{s0} \exp(-bP)$	[15]	5.8	680	0.876
3	$E_s(P) = E_{s0} \exp\left(-\frac{bP}{1-P}\right)$	[16]	2.6	384	0.798
4	$E_s(P) = E_{s0}\left(\frac{1-P}{1-bP}\right)$	[17]	-12.7	828	0.843
5	$E_s(P) = E_{s0}(1 - (1 + b)P + bP^2)$	[18]	1.5	331	0.790

Usually, a power dependence is used to describe deformation diagrams

$$\sigma = m\varepsilon^k, \quad (1)$$

where σ — mechanical stress, ε — relative deformation, m and k — numerical coefficients. The magnitude of the exponent of k is determined by the prevailing processes of the formation of the medium: the case of $k = 1$ corresponds to a purely elastic deformation (classical Hooke’s law), and the case of $k < 1$ corresponds to the deformation of the

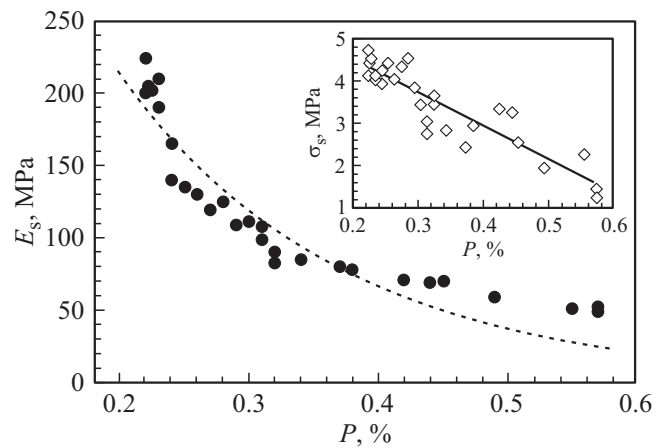


Figure 5. The dependence of the elastic modulus E_s on the porosity P according to compression test data. Dotted line — calculation by equation (2) from table. On the insert: the dependence of the tensile strength σ_s on porosity P .

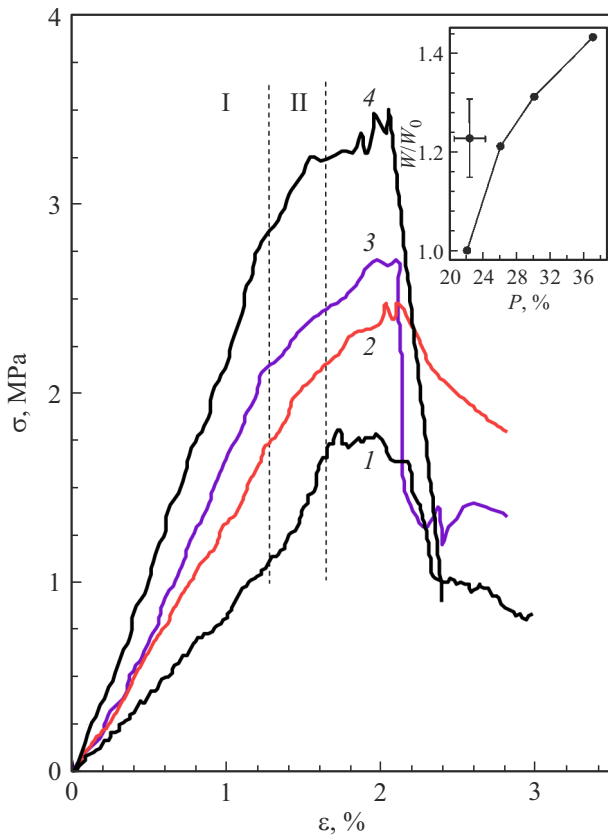


Figure 4. Compression diagrams of porous diatomite samples with different porosity P : 1 — 37%; 2 — 30%; 3 — 26%; 4 — 22%. In the insert: the dependence of the relative energy of AE signals on the porosity of samples. W_0 — AE signal energy for samples with porosity $P = 22\%$.

medium involving plastic deformation processes. In the case of predominance of pressing processes in the material, the value of the indicator $k > 1$. As before [11], to determine the exponent of k , the experimental data of compression diagrams were rearranged in logarithmic coordinates.

Studies have established that the curves in region I (Fig. 4) have the value $k > 1$, and in region II — $k < 1$. This confirms the predominance of deformation mechanisms associated with plastic deformation in this area (insert Fig. 3). In addition, it was found that for porosity values $P < 35\%$, the deformation pattern of the samples does not fundamentally change. With large porosity values, deviations from the observed regularity are possible.

According to experimental data of compression diagrams, the dependence of the static tensile strength of σ_s on porosity was obtained. As expected, with increasing porosity, the tensile strength decreases $\frac{\Delta\sigma_s}{\Delta P} = -9.8$ MPa.

To further confirm the dynamics of the destruction of ceramics based on diatomite, the AE method was used. It is known [19–21], that the growth or closure of micro- and macro-cracks, the collapse of pores, twinning processes, movement and exit to the grain boundaries of dislocations

and their clusters can act as sources of AE in such materials. It has been repeatedly noted [22,23] that AE is more pronounced the more heterogeneous the material is. In heterogeneous material, defects in the process of load (temperature) growth they are activated and are able to emit AE signals before the onset of macro-destruction [24].

AE during deformation and destruction of porous natural materials can be conditionally divided into discrete and continuous [25]. The discrete one refers to AE, whose signals consist of separate acoustic pulses. The continuous wave field, which is recorded as a single continuous signal, is a continuous acoustic emission signal.

It is considered [24,25] that the predominant source of the actually recorded AE in porous natural materials is the process of abrupt growth of cracks. To confirm the key role of crack formation and development in porous diatomite, AE processes were recorded simultaneously with the deformation process by compression of the sample. To do this, the AE signal taken directly from the piezo sensor is synchronized with the compression diagram (Fig. 2). It is easy to see that the most intense signal $U_d(t)$ of the deformable sample occurs during the formation and development of cracks in the sample. In our studies, it was found that the intensity of AE signals increases with increasing porosity of samples (insert in Fig. 4). The insert of Fig. 2 shows a view of the sample after deformation.

Figure 3 shows the spectral composition of AE (lies in the range $f = 0.2\text{--}8$ Hz), which occurs during the deformation of the sample. Like in [22], AE corresponded to the characteristics of „crackling noise“. There are a number of independent experimental studies [23–25], indicating that the distribution of time intervals between successive AE events in porous ceramic heterogeneous materials has the following form

$$N(t) = t^{-\gamma}, \quad (2)$$

where $N(t)$ — the distribution function of the duration of time intervals t between consecutive events AE; γ — dimensionless exponent. Numerous studies conducted on our samples with a porosity of $P = 35\text{--}40\%$ have shown that the distribution of time intervals between consecutive AE events $N(t)$ obeys the regularity (2) with a coefficient of $1.4 < \gamma < 1.8$. This is consistent with the data of [22,24], where the value of the exponent of the power law $\gamma \approx .4$ was recorded in the study of synthetic microporous silicon oxide and porous glass based on SiO_2 . A detailed study of the dependence of γ on the porosity of our material will be the subject of separate consideration.

4. Conclusion

Thus, the paper studies the deformation behavior of m processes of destruction of porous ceramics based on diatomite porous ceramics based on diatomite with porosity 20–60%. The results of the study showed a strong dependence of the elastic modulus of the material on

porosity: thus, with a porosity of 25%, the value of the elastic modulus was $E_s = 240$ MPa. An increase in the porosity of the medium by 2.5 times contributes to a fivefold decrease in the value of E_s . The dependence of the tensile strength of the material σ_s on porosity has also been experimentally recorded: with increasing porosity, the tensile strength decreases by $|\frac{\Delta\sigma_s}{\Delta P}| = 9.8$ MPa in the range under consideration is P . The results obtained will be useful in the development of new porous materials in terms of the relationship between the stress-strain state and the nature of the resulting damage in the volume and on the surface of the material.

Acknowledgments

The authors are grateful to Professor S.G. Kalenkov for the interest and stimulating discussions during the performance of this work.

Funding

The work was carried out within the framework of the state assignment of the Ministry of Education and Science to universities (project No. FZRR-2020-0023/ code 0699-2020-0023).

Conflict of interest

The authors declare that they have no conflict of interest.

References

- [1] P.S. Liu, G.F. Chen. Porous Materials: Processing and Applications. Elsevier Inc. (2014). 559 p.
- [2] X. Li, L. Yan, Y. Zhang, X. Yang, A. Guo, H. Du, F. Hou, J. Liu. Ceram. Int. **48**, 7, 9788 (2022).
- [3] S.V. Panin, P.S. Lyubutin, S.P. Buyakova, S.N. Kulkov. Phys. Mesomech. **12**, 3–4, 141 (2009).
- [4] F. Wang, Z. He, Z. Xie, S. Zhou. J. Chin. Ceram. Soc. **50**, 6, 1566 (2022).
- [5] S. Lyu, T. Zhao, Y. Wang, H. Han, T. Li, C. Zhang, D. Li, J.-K. Wang, J. Huang, P. Yu, D. Sun. Ceram. Int. **48**, 16, 22845 (2022).
- [6] A. Amoda, L. Borkiewicz, A. Rivero-Müller, P. Alam. Mater. Today Commun. **24**, 100923 (2020).
- [7] A.D. Dalgic, D. Atila, A. Karatas, A. Tezcaner, D. Keskin. Mater. Sci. Eng. C **100**, 735 (2019).
- [8] A.D. Kashin, M.B. Sedelnikova, V.V. Chebodaeva, P.V. Uvarkin, N.A. Luginin, E.S. Dvilis, O.V. Kazmina, Yu.P. Sharkeev, I.A. Khlusov, A.A. Miller, O.V. Bakina. Ceram. Int. (2022). In press.
- [9] P.J. Lopez, J. Desclés, A.E. Allen, C. Bowler. Current Opinion. Biotechnology **16**, 2, 180 (2005).
- [10] P. Pandit, P. Rananaware, A. D'Souza, M.D. Kurkuri, V. Brahmkhatri. J. Porous Mater. (2022). In print.
- [11] A.A. Skvortsov, M.N. Luk'yanov, I.E. Chebeneva, A.A. Skvortsova. Tech. Phys. Lett. **47**, 2, 166 (2021).
- [12] Y.E. Pivinskii, P.V. Dyakin. Refractories. Industrial Ceram. **56**, 3, 296 (2015).

- [13] A.V. Lavrov, V.L. Shkuratnik. *Acoustical Phys.* **51**, Suppl. 1, S2 (2005).
- [14] M. Kopec, S. Józwiak, Z.L. Kowalewski. *Mater.* **13**, 12, 2821 (2020).
- [15] W. Pabst, E. Gregorova. *Ceram. — Silikáty* **48**, 1, 14 (2004).
- [16] D.P.H. Hasselman. *J. Am. Ceram. Soc.* **45**, 9, 452 (1962).
- [17] R.L. Coble, W.D. Kingery. *J. Am. Ceram. Soc.* **39**, 11, 377 (1956).
- [18] A.F. Fedotov. *Vestn. Samara State Technical University Ser. Tekh. nauki* **4**, 40, 83 (2013). (in Russian)
- [19] V.L. Gilyarov, E.E. Damaskinskaya. *FTT* **63**, 6, 783 (2021). (in Russian)
- [20] G. Feng, J. Zhao, H. Wang, Z. Li, Z. Fang, W. Fan, P. Yang, X. Yang. *Powder Technol.* **396**, Part A, 449 (2022).
- [21] B. Casals, K.A. Dahmen, B. Gou, S. Rooke, E.K.H. Salje. *Sci. Rep.* **11**, 1, 5590 (2021).
- [22] E.K.H. Salje, D.E. Soto-Parra, A. Planes, E. Vives, M. Reinecker, W. Schranz. *Phil. Mag. Lett.* **91**, 8, 554 (2011).
- [23] E.K.H. Salje, H. Liu, L. Jin, D. Jiang, Y. Xiao, X. Jiang. *Appl. Phys. Lett.* **112**, 5, 054101 (2018).
- [24] G.F. Nataf, P.O. Castillo-Villa, J. Baró, X. Illa, E. Vives, A. Planes, E.K.H. Salje. *Phys. Rev. E* **90**, 2, 022405 (2014).
- [25] A.V. Lavrov, V.L. Shkuratnik. *Akust. Zhurn.* **51** (Appendix), 6 (2005). (in Russian)